

EFFECT OF FIBERS AND DISTRIBUTED NET REINFORCEMENT ON FRACTURE AND SIZE EFFECT IN CONCRETE STRUCTURES

Zdeněk P. Bažant*, Mohammad Rasoolinejad†, Abdullah Dönmez‡ AND Wen Luo§

*Northwestern University
Evanston, IL USA
e-mail: z-bazant@northwestern.edu

†Northwestern University
Evanston, IL USA
e-mail: Rasoolinejad@u.northwestern.edu

‡Istanbul Technical University, Istanbul, on postdoctoral appointment at Northwestern University
e-mail: donmezab@itu.edu.tr

§Northwestern University
Evanston, IL USA
e-mail: wenluo2016@u.northwestern.edu

Key words: Size Effect, Fracture Mechanics, Fiber Reinforced Concrete, Brittleness, Finite Element Analysis, Projectile Impact

Abstract. The size effect in geometrically similar notched and unnotched FRC specimens of different fiber contents is simulated computationally using the FE crack band model coupled with the microplane constitutive model M7f for fiber reinforced concrete (FRC), which was previously calibrated by extensive material test data. The impact and penetrations of projectiles into FRC walls is also studied. It is found that, for any level of fiber volume ratio, the size effect exists and is pronounced. The fiber reinforced concrete specimens show considerably higher fracture energy than the plain ones.

1 INTRODUCTION

In the microplane constitutive material model, the post-peak softening in a representative volume of material is characterized in terms of vectors rather than tensors. The vectorial form has an important advantage. It makes it possible to relate the microplane deformations to microcrack opening, frictional slip, fiber pullout and possible fiber breakage. Microplane model M7f extended to FRC with short discontinuous fibers was developed at Northwestern University [1, 2]. It was demonstrated to fit well the main material tests reported for FRC. In FraMCoS article, the M7f model is employed

to study two underexplored problems of FRC—the role of fibers in the energetic size effect of quasibrittle fracture mechanics, and in the penetration of projectiles into FRC walls.

The high tensile strength of steel fibers enhances the tensile behavior of FRC [3–5]. The steel fibers also enhance ductility and provide good dynamic response to the FRC [5]. The fibers also could capture early age cracking due to shrinkage [6, 7].

2 SIZE EFFECT

Two causes of size effect must be distinguished—statistical (first properly char-

acterized by Weibull in 1939), and energetic (discovered in 1984 [8, 9]). The latter dominates for reinforced concrete and is the only one studied in this lecture. The size effect is of two types, described by equations:

$$\sigma_N = \sigma_0 \left(1 + \frac{rD_b}{D}\right)^{1/r} \quad (\text{Type 1}) \quad (1)$$

$$\sigma_N = Bf'_t \left(1 + \frac{D}{D_0}\right)^{-1/2} \quad (\text{Type 2}) \quad (2)$$

where σ_N is the nominal strength of structure (load divided by characteristic cross section area), and $\sigma_0, D_b, r, Bf'_t, D_0$ are constants. The latter [8–10] dominates for reinforced concrete and is purely energetic. It is caused by the stored energy release due to large stable crack growth [11–13]. Type I occurs for plain (unreinforced concrete), in which the structure becomes unstable as soon as a continuous macrocrack starts growing from a finite damaged microcracking zone, and is caused by stress redistribution [10, 14]. For very large sizes, Type 1 transits to Weibull statistical size effect [15] (which is omitted from Eq. (1) and is not discussed here). The Type 2 size effect factor, Eq. (2), has just been adopted for the 2019 revision of the ACI code (Standard 318/2019)—for beam shear, slab punching, and compressions struts of strut-and-tie model.

3 RESULTS

A set of scaled three-point bending test has been simulated and analyzed. The beam depth D is considered as characteristic size. The span is $4D$. The beams had notches at mid-span up to the quarter depth of the beam. The scaled specimens included $D = 400, 800, 1600$ and 3200 mm. The same scaling was considered for all the fiber volume ratios. In total, 16 models have been built. Their tests were simulated by FE crack band model [16], in which the element size was the same for all the specimen sizes, to prevent spurious mesh sensitivity. The M7 parameters have been calibrated to capture the FRC test reported by Li et al. [5] (Fig. 1). They performed the uniaxial tensile test on the $350 \times$

100×20 mm prisms. Various fiber types have been used, but here we consider only Dramix steel fibers. The fiber volume ratios were 0, 2, 3 and 6 percent, respectively. The curves of stress versus normalized deflection are plotted in Fig. 2.

The measurements of size effect in notched fracture specimens can be exploited to identify the fracture energy, G_f , and the characteristic fracture process zone size, c_f , of FRC. To this end, the Type 2 SEL is related to equivalent linear elastic fracture mechanics (LEFM) and is converted to the linear regression plot [9, 10, 15]:

$$Y = AX + C \quad (3)$$

$$\text{where } X = D, \quad Y = \frac{1}{\sigma_N^2} \quad (4)$$

$$\text{and } A = \frac{g(\alpha)}{EG_f}, \quad C = c_f \frac{g'(\alpha)}{EG_f} \quad (5)$$

Here E is the Young's elastic modulus and $g(\alpha)$ is the dimensionless energy release function of LEFM. Fig. 3 presents the regression plots of the computed Y versus X , for various sizes D and various fiber contents. Based on these regressions, one obtains $G_f = 279, 2424, 2491, 3994$ N/m for fiber contents 0, 2%, 3% and 6%, respectively. It may be concluded that adding fiber raises the fracture energy dramatically.

The calculated size effect plots of $\log \sigma_N$ versus $\log D$ are shown in Fig. 4 for fiber contents 0, 2%, 3% and 6%, and for four different specimen sizes (or depths) $D = 400, 800, 1600$ and 3200 mm. The SEL curves (solid lines) are seen to fit the data points from the FE simulations very well. It may be noted that, in these notched fracture specimens, the fibers significantly increase the maximum load. This is not what is observed in the compression tests of standard unnotched test cylinders. It is also interesting that, based on the simulations, the fiber content has no clearly definable effect on the transitional size D_0 of the size effect law.

The role of fibers in the Type 1 size effect of FRC has also been simulated. The plain concrete and the 2% FRC exhibited Type 1 size effect while 3% and 6% FRC did not. The

load-displacement curve in unnotched specimens reached a plateau for 3% and 6% FRC, and the maximum nominal stress became independent of the size.

Another point of keen interest is the effect of fibers on the resistance to impact. As previously found at Northwestern [17–19], the comminution (or fine fragmentation) of material during penetration of projectiles through concrete has a great damping effect, decelerating the projectile, reducing penetration depth and, in the case of full penetration, reducing the exit velocity of the projectile. This comminution effect, which bears some interesting analogy with the theory of turbulence, is documented by comparisons with test data seen Fig. 5a. They show that, without the comminution effect, the test results cannot be matched. The graphs show the dependence of the exit velocity of the projectile on the thickness of the perforated slab.

Most studies concluded that FRC does not significantly reduce the penetration depth, but is very effective for reducing the crack width [20–24]. Fig. 5b shows that the projectile exit velocity causes only a slight penetration depth reduction as fiber is added to the concrete beyond the 2% fiber content. More results will be available by time of the conference.

4 CONCLUSIONS

1. Prediction of the size effect in fiber reinforced concrete structures requires fracture mechanics.
2. For all the steel fiber percentages analyzed, type II size effect was observed in the notched three-point bend tests.
3. Fiber pullout near the crack tip causes gradual postpeak softening on the load-displacement curves of three point bend tests.
4. The fiber reinforcement neither diminishes nor enhances the size effect of Type 2.
5. The fiber reinforcement does not have a

noticeable effect on the transitional size of the size effect curve.

6. The values of fracture energy of FRC identified by the size effect method from the computed maximum loads of scaled notched specimens demonstrate that introducing fibers into concrete and increasing their content causes the fracture energy to increase dramatically.
7. Compared to concrete without fibers, short fiber reinforcement significantly increases the maximum loads in Type 2 failure of notched fracture specimens. It is inferred that it also significantly increases the maximum loads of structures failing only after large stable crack growth (as in shear of RC beams).

Note: Details of the specimen and material properties and of calculations will be given in a separate refereed journal article under preparation.

Acknowledgment: Partial funding under ARO grant W911NF-19-1-0039 to Northwestern University is gratefully appreciated.

REFERENCES

- [1] Ferhun C Caner, Zdeněk P Bažant, and Roman Wendner. Microplane model m7f for fiber reinforced concrete. *Engineering fracture mechanics*, 105:41–57, 2013.
- [2] Ferhun C Caner and Zdeněk P Bažant. Microplane model M7 for plain concrete. i: Formulation. *Journal of Engineering Mechanics*, 139(12):1714–1723, 2012.
- [3] J Feng, WW Sun, XM Wang, and XY Shi. Mechanical analyses of hooked fiber pullout performance in ultra-high-performance concrete. *Construction and Building Materials*, 69:403–410, 2014.
- [4] Jun Feng, Weiwei Sun, Zhilin Liu, Chong Cui, and Xiaoming Wang. An armour-piercing projectile penetration in a double-layered target of ultra-high-performance

- fiber reinforced concrete and armour steel: Experimental and numerical analyses. *Materials & Design*, 102:131–141, 2016.
- [5] Zongjin Li, Faming Li, TY Paul Chang, and Yiu-Wing Mai. Uniaxial tensile behavior of concrete reinforced with randomly distributed short fibers. *Materials Journal*, 95(5):564–574, 1998.
- [6] Jun Zhang and Victor C Li. Influences of fibers on drying shrinkage of fiber-reinforced cementitious composite. *Journal of engineering mechanics*, 127(1):37–44, 2001.
- [7] Mohammad Rasoolinejad, Saeed Rahimi-Aghdam, and Zdeněk P Bažant. Prediction of autogenous shrinkage in concrete from material composition or strength calibrated by a large database, as update to model b4. *Materials and Structures*, 52(2):33, 2019.
- [8] Zdeněk P Bažant. Size effect in blunt fracture: concrete, rock, metal. *Journal of engineering mechanics*, 110(4):518–535, 1984.
- [9] Zdenek P Bažant and MT Kazemi. Determination of fracture energy, process zone length and brittleness number from size effect, with application to rock and concrete. *International Journal of fracture*, 44(2):111–131, 1990.
- [10] Zdenek P Bazant and Jaime Planas. *Fracture and size effect in concrete and other quasibrittle materials*, volume 16. CRC press, 1997.
- [11] Abdullah Dönmez and Zdeněk P Bažant. Size effect on punching strength of reinforced concrete slabs with and without shear reinforcement. *ACI Structural Journal*, 114(4):875–886, 2017.
- [12] Mohammad Rasoolinejad and Zdeněk P Bažant. Size effect of squat shear walls extrapolated by microplane model M7. *ACI Structural Journal*, page in press, 2019.
- [13] Ferhun C Caner, A Abdullah Dönmez, Sıddık Şener, and Varol Koç. Double cantilever indirect tension testing for fracture of quasibrittle materials. *International Journal of Solids and Structures*, 162:76–86, 2019.
- [14] Zdenek P Bazant, Isaac M Daniel, and Zhengzhi Li. Size effect and fracture characteristics of composite laminates. *Journal of engineering materials and technology*, 118(3):317–324, 1996.
- [15] Zdenek P Bazant and Jia-Liang Le. *Probabilistic mechanics of quasibrittle structures: strength, lifetime, and size effect*. Cambridge University Press, 2017.
- [16] Zdeněk P Bažant and Byung H Oh. Crack band theory for fracture of concrete. *Matériaux et construction*, 16(3):155–177, 1983.
- [17] Zdeněk P Bažant and Ferhun C Caner. Impact comminution of solids due to local kinetic energy of high shear strain rate: I. continuum theory and turbulence analogy. *Journal of the Mechanics and Physics of Solids*, 64:223–235, 2014.
- [18] Ferhun C Caner and Zdeněk P Bažant. Impact comminution of solids due to local kinetic energy of high shear strain rate: II—microplane model and verification. *Journal of the Mechanics and Physics of Solids*, 64:236–248, 2014.
- [19] Wen Luo, Viet T Chau, and Zdeněk P Bažant. Effect of high-rate dynamic comminution on penetration of projectiles of various velocities and impact angles into concrete. *International Journal of Fracture*, pages 1–11, 2019.
- [20] WF Anderson, AJ Watson, and PJ Armstrong. Fiber reinforced concretes for the protection of structures against high

- velocity impact. *Structural Impact and Crashworthiness*, 2:687–695, 1984.
- [21] EF O'Neil, BD Neeley, and JD Cargile. Tensile properties of very-high-strength concrete for penetration-resistant structures. *Shock and Vibration*, 6(5-6):237–245, 1999.
- [22] Avraham N Dancygier, David Z Yankelevsky, and Chanoch Jaegermann. Response of high performance concrete plates to impact of non-deforming projectiles. *International Journal of Impact Engineering*, 34(11):1768–1779, 2007.
- [23] AN Dancygier and DZ Yankelevsky. High strength concrete response to hard projectile impact. *International Journal of Impact Engineering*, 18(6):583–599, 1996.
- [24] MH Zhang, VPW Shim, G Lu, and CW Chew. Resistance of high-strength concrete to projectile impact. *International Journal of Impact Engineering*, 31(7):825–841, 2005.

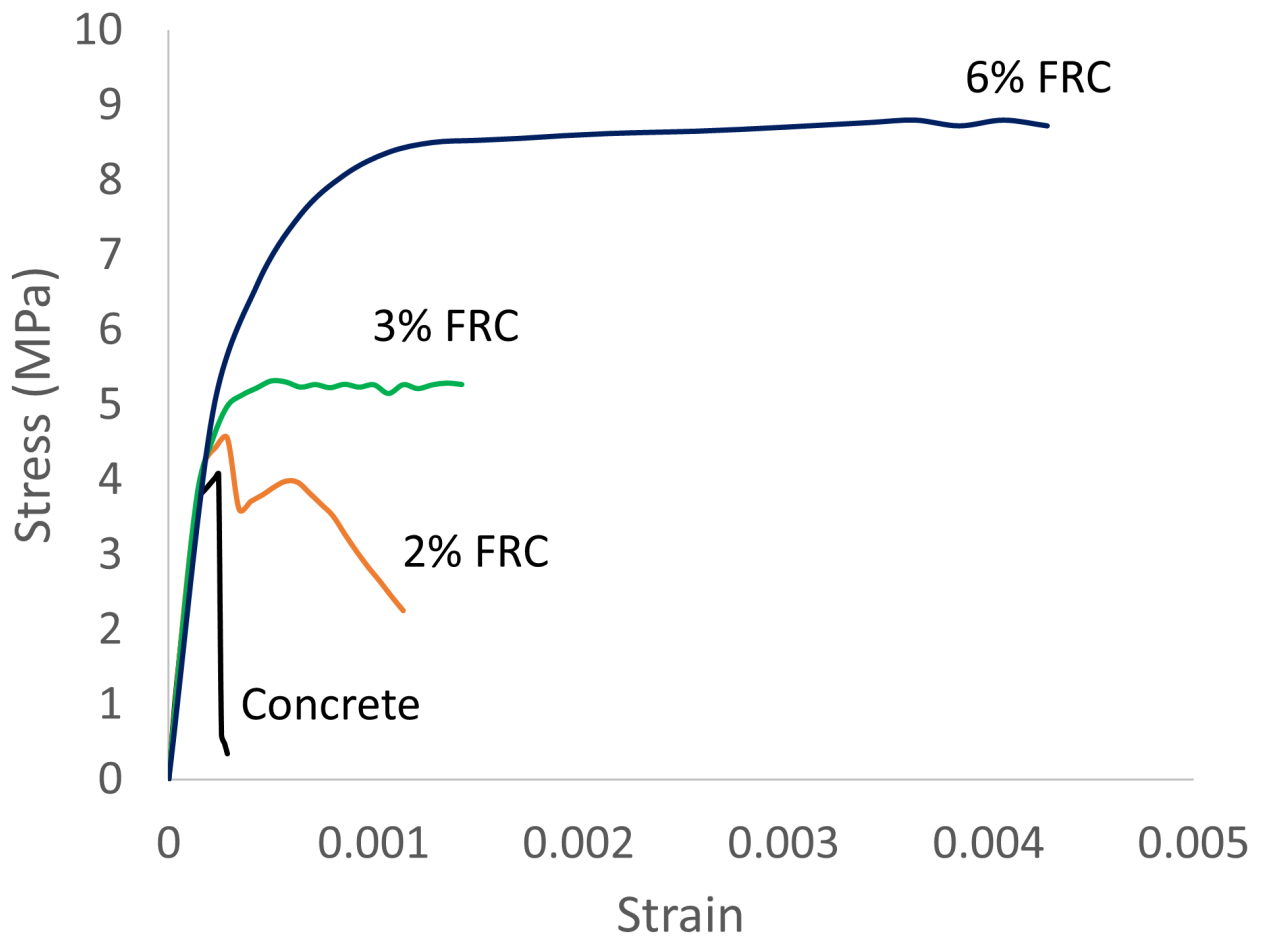


Figure 1: Stress-strain curves of FRC calibrated by M7-fiber based on the tests by Li et al. [5]

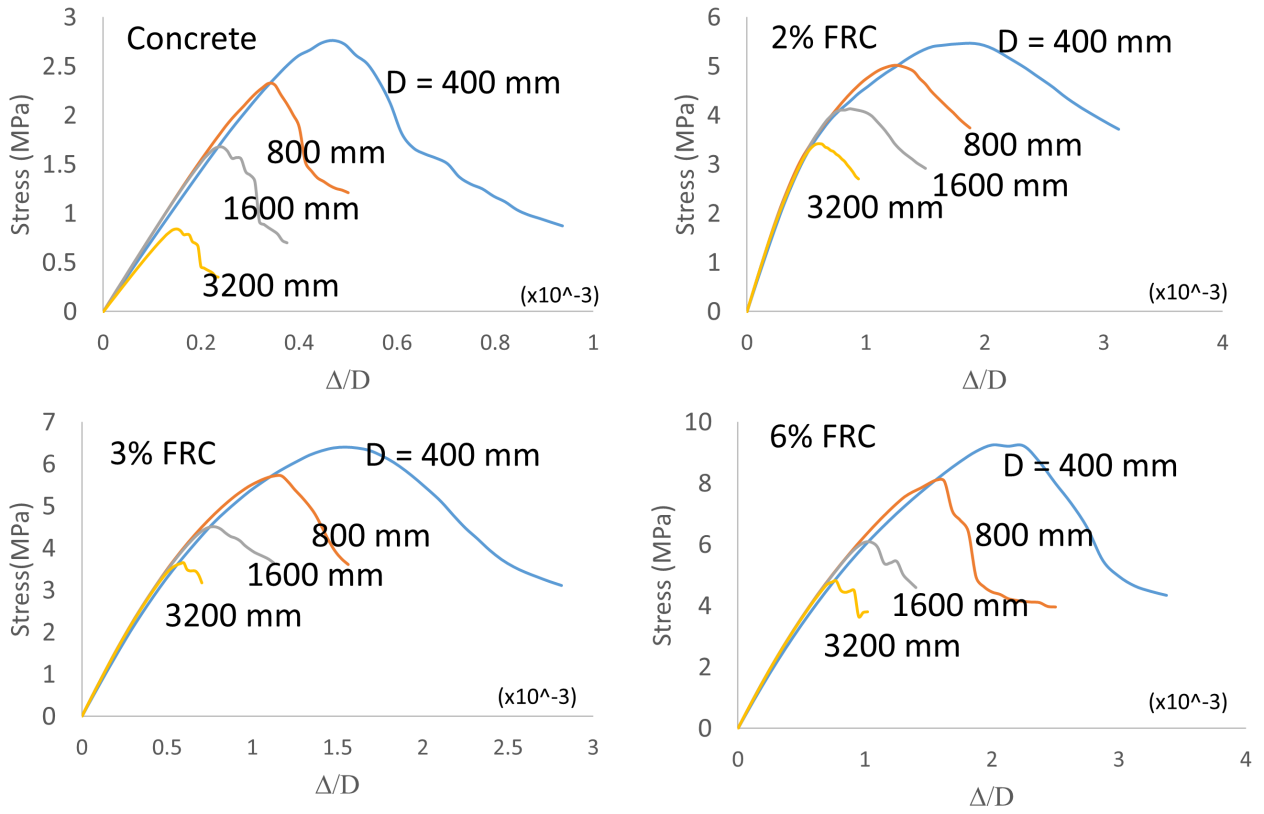


Figure 2: Three-point bending stress-strain curves

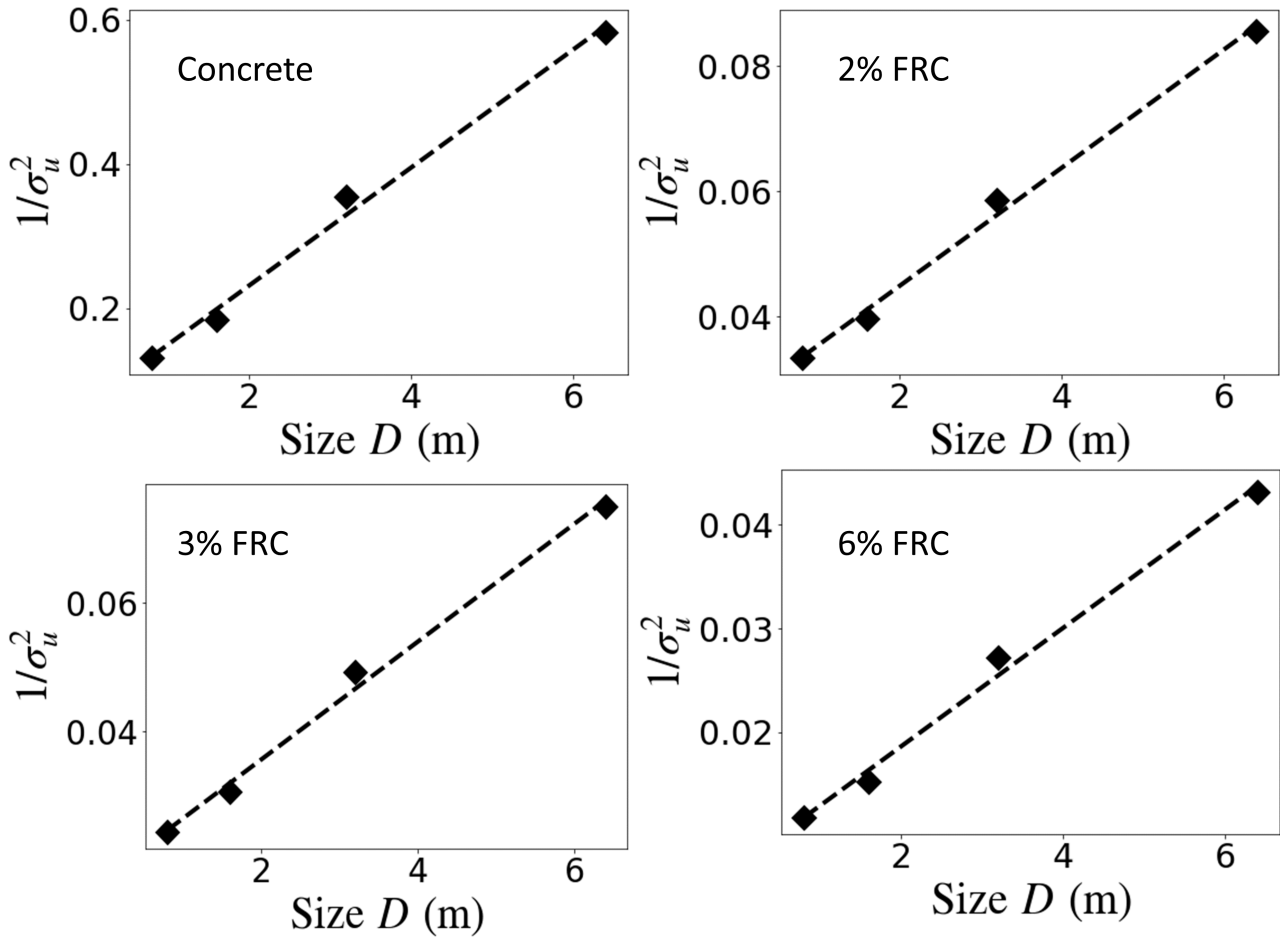


Figure 3: Linear regression size effect plots

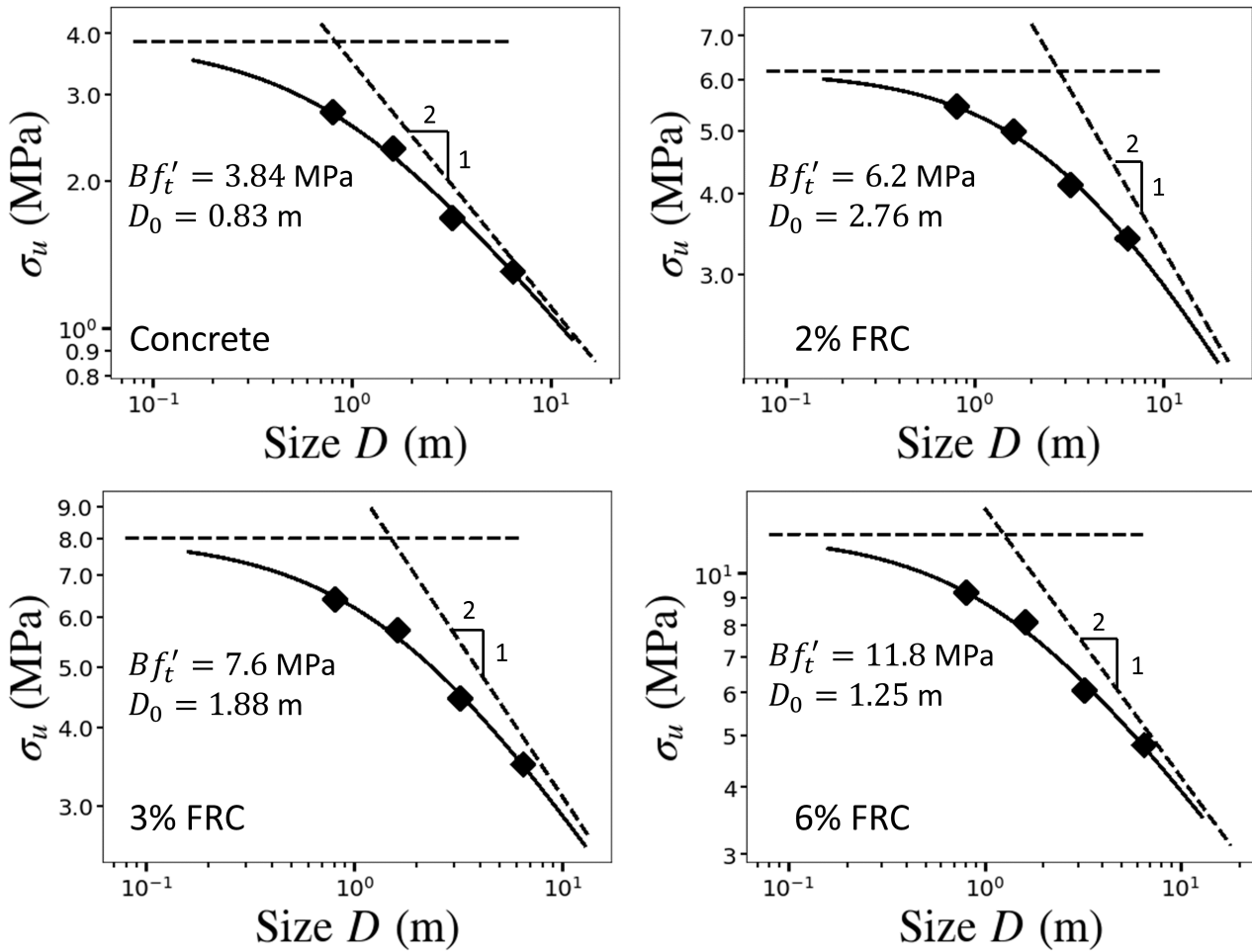


Figure 4: Size effect plots of FRC in logarithmic scale

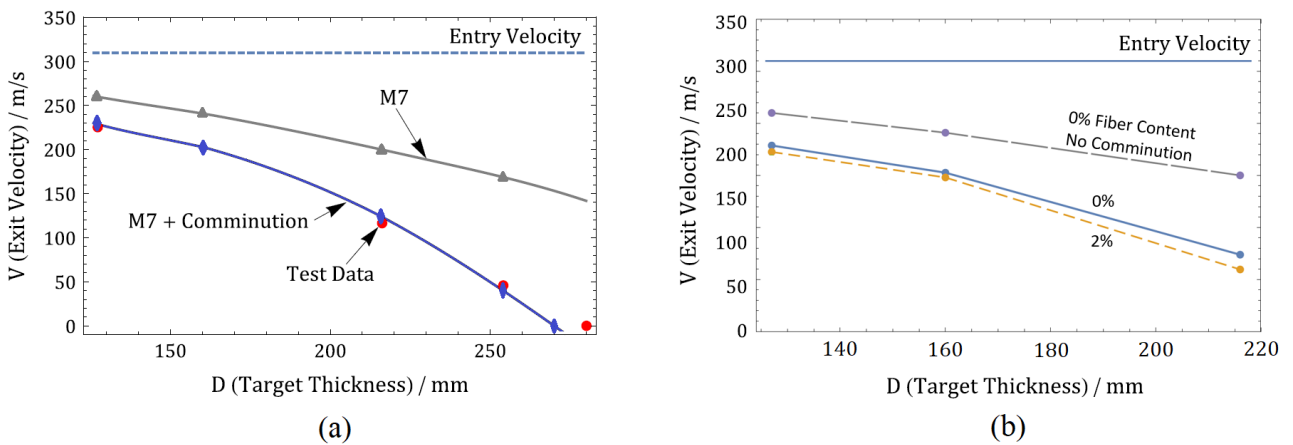


Figure 5: Projectile impact with and without material comminution, for concrete with and without fibers